Manuscript

Understanding sex-related differences in cardiac energy metabolism through genome-scale metabolic models in patients with dilated cardiomyopathy

Giorgia Del Missier [1,‡], Hannah Schultheiß [2,‡], Michal Skawinski [3,‡] and Xenia Sterl [4,‡]

[1] Faculty of Science and Engineering, Maastricht University; g.delmissier@student.maastrichtuniversity.n
[2] Faculty of Science and Engineering, Maastricht University; h.schultheiss@student.maastrichtuniversity.nl
[3] Faculty of Science and Engineering, Maastricht University; m.skawinski@student.maastrichtuniversity.nl
[4] Faculty of Science and Engineering, Maastricht University; x.sterl@student.maastrichtuniversity.nl
‡ These authors contributed equally to this work.

Abstract: Dilated cardiomyopathy (DCM) is characterized by left- or biventricular dilation, making the cardiac muscle thin and friable which ultimately results in heart failure as the pumping ability of the heart is reduced. Recent evidence suggests that alterations in energy metabolism are related to the development of DCM. Specifically, it is thought that the heart undergoes a loss of metabolic flexibility leading to reduced ATP production with a shift from fatty acid oxidation (FAO) to glycolysis. Generally, males show a higher incidence and severity of DCM as compared to females. However, little is known about sex-related differences occurring in DCM, especially with regards to cardiac energy metabolism. This study used differential gene expression analysis and gene set enrichment analysis to identify enriched metabolic pathways in male and female DCM patients. Afterwards, the exact differences in the identified pathways were further investigated using context-specific genome-scale metabolic models (GEMs). Initial inspection of the models revealed that female DCM patients had more active pathways mostly belonging to fatty acid oxidation (FAO), glutamate metabolism and glycolysis. These findings were then further confirmed using Flux Variability Analysis (FVA), as some reactions only carried flux in the female DCM model. Moreover, FVA showed that some metabolic pathways in male DCM patients resembled those of females, potentially implying a 'feminization' of the male heart in DCM. Nevertheless, a major limitation of the current study is that, to the best of our knowledge, no in vivo studies exist that investigated sex differences in cardiac energy metabolism. While this hampered the validation of the observed results, it also highlights the importance of conducting studies like the one at hand to further elucidate sex-related differences in the pathology of DCM.

Keywords: heart failure; dilated cardiomyopathy; sex differences; RNAseq; cardiac energy metabolism; genome-scale metabolic models; flux variance analysis; flux space sampling;

Figures and tables: attached below references. In total 6 figures and 1 table.

Supplementary materials: attached at the end of document. In total 4 tables.

Number of Words - Abstract: 279

Number of Words - Main Part: 3994

Maastricht University
Faculty of Science and Engineering
Masters Systems Biology
PRO4002

1. Introduction

Cardiomyopathies are heart muscle disorders that cause mechanical and/or electrical dysfunction of the heart. One type of cardiomyopathy is dilated cardiomyopathy (DCM), a non-ischemic disorder that is caused by structural and functional abnormalities of the myocardium. Specifically, DCM is characterized by left- or biventricular dilation, which results in a weakened and thin cardiac muscle with decreased pumping ability, effectively reducing the flow of oxygenated blood throughout the body [1,2].

After coronary heart disease, dilated cardiomyopathy is the most common cause of heart failure [3], with an estimated incidence of approximately one out of 250 people [4,5]. Moreover, it is the most common indication for heart transplantation worldwide [6].In general, males show a higher incidence and severity of DCM as compared to females [7]. However, little is known about sex differences occurring in DCM [3]. A study by Haddad et al. (2008) [8] showed that there is a sex-specific genetic expression profile for DCM: genes found to be deregulated specifically in females are usually involved in energy metabolism and regulation of transcription and translation, whereas deregulated genes in males are related to muscular contraction. Moreover, another study found that men with DCM showed a higher expression of apoptosis-related proteins than women with DCM [9].

Recent evidence suggests that impairments in energy metabolism are related to the pathogenesis of DCM. Specifically, the genetic expression of metabolic pathways of mitochondria and the production of ATP is altered in DCM patients when compared to a healthy control [1]. Failing hearts undergo what is known as loss of metabolic flexibility, a term that defines the ability of the myocardium to produce ATP from different substrates depending on their availability. In a normal functioning heart, fatty acid oxidation (FAO) is the biggest contributor to ATP production (40-60%), while glucose metabolism accounts for the remaining 20-40%. In a DCM heart, there is a shift towards glycolysis and ketone oxidation to produce ATP [10]. The reduction of metabolic flexibility, together with an increased production of reactive oxygen species (ROS) due to increased oxidative stress, affects cardiac contractility and ATP production [11]. On average, considering all causes of cardiac metabolic impairment, it was estimated that the production of ATP is reduced by 30-40% in DCM hearts [10].

Another research by Alexander et al. (2010) [12] found evidence of sex-related differences in DCM patients in the levels of plasma metabolites such as cortisol, cortisone and androgen. In this study, significant differences in metabolite concentrations were found between males and females in healthy controls while DCM patients did not show differences

between sexes for the same metabolites. This would imply a metabolic 'feminization' of the cardiac tissue in males with DCM.

Despite these findings, there remains some paucity about the exact sex-specific differences in cardiac energy metabolism in DCM patients. A powerful tool to identify metabolic variation occurring in diseases is provided by in silico genome-scale metabolic models (GEMs), as they do not require any kinetic information about the reactions and are thus less computationally expensive [13,14]. Therefore, in this study, we want to investigate sex-related differences in patients with DCM using context-specific GEMs. First, we will use differential gene expression analysis to determine which genes are differentially expressed in males and females with DCM. Next, we will use these results in gene set enrichment analysis (GSEA) to identify enriched metabolic pathways. We will then investigate what the exact differences in these pathways are between males and females with DCM using context-specific GEMs and mathematical approaches such as Flux Variability Analysis (FVA) and Flux Space Sampling (FSS).

2. Methods

2.1. Data

The data employed in this study was obtained from a publicly available dataset of the MAGNet consortium (BioProject: PRJNA595151 [15]) containing the RNA sequencing data from 366 biopsies of left ventricular free-wall tissue collected during cardiac surgery from subjects suffering from heart failure and from unused donor hearts with apparently normal function. 166 (66 females) out of the 366 samples were collected from dilated cardiomyopathy (DCM) patients and 166 (89 females) from the unused donor hearts, serving as a control in this study. Metadata (age, gender, ethnicity) about each sample was also available. Analysis on sample characteristics and principal component analysis (PCA) were performed in R using tidyverse [16] and pcaMethods [17] packages respectively.

2.2. Data Pre-processing and Exploration

Prior to analysis, the log2-transformed Counts Per Million (CPM) values of the data set were normalized using the Trimmed Means of Means (TMM) normalization method in R using the edgeR [18] and limma [19] packages in version 3.14 of Bioconductor, which has been found to perform well in comparative studies [20]. The method involves the calculation of sample-specific normalization factors which are then used to calculate the

between-sample normalized log2-transformed CPM values for each gene and sample.

2.3. Differential Expression Analysis

A method that can be used to determine which genes are expressed at different levels between conditions is Differential Expression (DE) analysis. A common first step in DE analysis is the filtering of genes that consistently have zero or low counts [21]. Here, the function filterByExpr of the edgeR package was used. As a next step, linear modeling followed by empirical Bayes statistical modeling of the aforementioned pre-processed RNA-seq data was performed in R using the limma package [22]. DE analysis was performed between DCM and Donor samples for females and males separately, obtaining two log fold change values for each gene. Gene annotations were retrieved using the bioMart package [23] from the Ensembl database, using the GRCh38.p13 version of the Homo Sapiens genome.

2.4. Gene Set Enrichment Analysis

Gene Set Enrichment Analysis (GSEA) is a computational method that can identify which pathways are enriched in a pre-defined ranked gene list and whether there are significant differences between two biological states.

The input for GSEA was thus a CSV file containing the gene names, together with the corresponding log fold change and p-value, obtained from the DE analysis for the tested conditions, i.e. DCM vs control in males and females separately.

The analysis was performed twice, using two different databases for enrichment analysis: the Kyoto Encyclopedia of Genes and Genomes (KEGG) and WikiPathways. In both cases, adjustment for multiple testing was performed using the Benjamini-Hochberg procedure. The final output of the analysis were the pathways that were found to be enriched only in males or females.

2.5. Context Specific Genome-Scale Metabolic Models

Based on the results obtained from the GSEA, it was decided to further investigate the differences in female and male cardiac energy metabolism in DCM. Genome-scale metabolic models represent all known metabolic reactions with a stoichiometric matrix S, containing the stoichiometric coefficients for each reaction. Using the stoichiometric matrix and assuming that the system is under a steady-state, where the concentration of

each metabolite remains constant over time, fluxes through each reaction can be predicted [24]. All reaction fluxes that satisfy the steady-state assumption in the null space of S. By imposing constraints on some reactions, the null space can be further reduced, and different methods exist that allow for the analysis of the resulting solution space. This study made use of two different analysis techniques, namely Flux Variability Analysis (FVA) and Flux Space Sampling, which will be further discussed in Section 2.5.3 and 2.5.4, respectively.

2.5.1. Construction of Context-Specific GEMs

As mentioned previously, GEMs usually aim to include all known metabolic reactions. Clearly, not all of these reactions will be active in a specific cell type or under particular conditions. Therefore, various algorithms have been developed that allow for the construction of context-specific GEMs using mRNA expression data.

One such method is the Gene Inactivity Moderated by Metabolism and Expression (GIMME) algorithm which has been implemented in the Constraint-Based Reconstruction and Analysis (COBRA) toolbox (Version 3.0) in Matlab (Version 2021b) [25,26]. The required inputs for the algorithm are a set of gene expression data, a genome-scale reconstruction of the metabolic network and one or more Required Metabolic Functionalities (RMF) that the model is supposed to achieve. Based on these inputs, GIMME then determines the reactions that should be active based on a predefined threshold. Reactions with an expression level below that threshold will be deemed inactive and will only be added to the model if they are required to fulfill the objective function. To determine which of the inactive reactions will need to be added to the model, linear optimization methods are used [25].

For this study, four different models (Control female and male & DCM female and male) were created. To do so, the expression data of the MAGNet dataset was converted to FPKM values and the mean expression for each gene and group was calculated. For each model, the mean gene expression values were mapped to the corresponding reaction of the Recon3D model, which is a community-driven model, providing a comprehensible reconstruction of human metabolism [27].

Since one of the main objectives of a cardiac cell is to generate as much energy as possible, mostly in the form of ATP, the RMF of all models was set to maximize ATP production. The threshold defining reactions as (in)active was set to half a standard deviation above the mean, calculated from the expression values of all models (i.e., all models had the same threshold).

2.5.2. Quality Checks and Model Overview

To test for basic model functionality, sanity checks, following a script provided within the COBRA toolbox, were performed on all obtained models. To identify differences between the four models, two different overlays were created, showing the differences in retained reactions between the control male and female models, and DCM male and female models. The overlays were then visualized on the Recon3D map using the Virtual Metabolic Human (VMH) website [28].

2.5.3. Flux Variability Analysis

As aforementioned, multiple different reaction flux vectors exist that satisfy the objective function in the same way. Flux Variability Analysis (FVA) provides a way to account for the different possible solutions. Using linear programming, FVA finds the minimum and maximum fluxes through each reaction that are needed to fulfill the objective function [29].

In this study, FVA was performed on six subsystems of interest, namely citric acid cycle, pyruvate metabolism, glutamate metabolism, FAO, glycolysis/gluconeogenesis and oxidative phosphorylation, for each of the models. As this study was only interested in the sex-related differences in energy metabolism of DCM patients, only reactions that were either shown to have different flux ranges in the two control models, but not in the diseased models, or reactions with the same flux ranges in the control models, but not in the diseased models, were further investigated.

2.5.4. Flux Space Sampling

A disadvantage of FVA is that it needs an objective function to be specified, which introduces an observer bias about the main objective of the cell. A technique that does not require such an objective function is Flux Space Sampling (FSS). With this method, a sequence of feasible solutions is generated that fulfill the network constraints of a metabolic model. With enough samples, an accurate representation of the entire solution space can be created. This provides information on not only the range of feasible flux solutions, but also on their probability, unlike FVA.

To further investigate possible sex differences in metabolism in DCM patients, we were planning to perform FSS on the previously mentioned subsystems for each model. Unfortunately, when implementing the FSS algorithm, some technical difficulties were

encountered. Due to time constraints, this analysis could therefore not be performed successfully.

3. Results

3.1. Data Description

The total study population was composed of 332 samples (155 females). 66 out of the 155 female samples and 100 out of the 177 male samples were obtained from DCM patients. Table 1 shows a comparison of the baseline characteristics between men and women. Statistical analysis revealed that the observed frequency of African-American and Caucasian samples was significantly different (p-value < .001) between control and DCM samples in the female subpopulation, while no significant difference (p-value = 0.06) was detected for male samples. Similarly, age was found to be significantly different between female control and DCM samples (mean age 59 ± 12.5 years vs. 51.1 ± 11.7 years in female control vs DCM, respectively, $p < 0.001$). For men, the mean age was not significantly different between control and DCM (52.6 ± 12.2 years vs. 52.7 ± 9.8 years in male control vs. DCM, respectively, $p = 0.8$).

To further investigate how the detected significant differences in age and ethnicity in the female subpopulation affected the gene expression data and to determine whether they were confounders that needed to be corrected for, PCA plots were constructed. As none of the first 10 principal components separated the samples by ethnicity or age, it was decided that neither of these two variables was a confounder. Therefore, they were not corrected for in subsequent analysis.

3.2. Differential Expression Analysis

After filtering, 6746 genes were removed, leaving 14035 genes for further analysis. A total of 8429 differentially expressed genes (DEGs) (3685 upregulated and 4744 downregulated) were identified for female DCM samples when compared to donors and 6928 DEGs (2880 upregulated and 4048 downregulated) for male samples. 2240 upregulated DEGs were common between males and females (Figure 1A). Similarly, 2240 DEGs were found to be downregulated in male as well as female DCM patients (Figure 1B).

3.3. GSEA

In total, 53 pathways were found to be enriched using the KEGG database (23 for males and 32 for females) and 37 with WikiPathways (20 for males and 17 for females) (Supplementary Table 2). For both sexes and databases, most enriched pathways belonged

to the immune response, energetics and metabolism, and signal transduction (Figure 2). As it was then decided to further investigate sex-related differences in cardiac energy metabolism, the pathways belonging to the energy and metabolism category were further represented with dotplots (Figure 3). Common enriched pathways for both female and male DCM patients found with the KEGG database were: central carbon metabolism in cancer, glycerophospholipid metabolism, metabolic pathways and protein digestion and absorption. With WikiPathways the following pathways were found to be commonly enriched in male and female DCM patients: amino acid metabolism, conversion of angiotensinogen to angiotensin II and renin-angiotensin-aldosterone system(RAAS). All of the commonly enriched pathways were similarly enriched in males and females (i.e., had a similar gene ratio, enrichment score and p-value). Using the KEGG database, some pathways (i.e, retinol metabolism, glycolysis/gluconeogenesis, pyruvate metabolism) were found to be only significantly enriched in male DCM patients. For WikiPathways, the pathways that were only enriched for males were codeine and morphine metabolism and metabolic reprogramming in colon cancer. Here, one pathway (glycerophospholipid biosynthetic pathway) was also found to only be enriched in females.

3.4. GEMs - Model Overview

The results obtained from the sanity checks of the four created models can be found in the supplementary materials (Supplementary Tables 3 & 4). In Figure 4A and B, the differences in the retained reactions for the subsystems of interest between the control and DCM models can be seen respectively. For the differences in retained reactions between the female and male control models (Fig. 4A), it can be observed that most of the reactions were still present in both models (i.e., brown reactions). However, 17 reactions were only present in the male control model (i.e., blue reactions). One of these reactions belonged to pyruvate metabolism, three to glutamate metabolism and 17 to FAO. The names of the reactions that were only present in the male control model can be found in Supplementary Table 5. Interestingly, all of the reactions that were shown to be only present in the male control model were active in both (i.e., female and male) DCM models, indicating a potential change in active energy-related metabolic pathways in female DCM patients.

The overlay created for the two DCM models (Fig. 4B) again shows that most reactions were retained in both models. Nevertheless, 18 reactions were found to only be present in the female DCM model (i.e., yellow reactions). Three out of these reactions belonged to glycolysis and 15 to FAO. The names and descriptions of these reactions can be found in

Supplementary Table 5. None of these reactions was present in either of the two control models, again indicating a change in active metabolic pathways in female DCM patients.

3.5. GEMs - FVA

After performing Flux Variability Analysis on the subsystems for energy metabolism stated in Section 2.5.3, the reactions with flux ranges that showed differences only in the control groups or only in the diseased groups were retained for further analysis.
Thus, out of the six subsystems tested, only three showed some difference in the flux range vectors results: for the FAO subsystem, out of 614 reactions tested, 17 were found to be altered in one out of the four models (Figure 5, reactions labeled with "*"). Specifically, six out of the 17 reactions only showed a different flux range in the male control model, possibly indicating a metabolic change in male DCM patients. The remaining 11 reactions did not carry a flux in any model, except for the female DCM one. In the pyruvate metabolism subsystem, 5 of the 22 reactions had a difference in the flux range vectors (Figure 5, reactions labeled with "**"). Here, similar observations like for FAO can be made. Four reactions only carried a flux in the female DCM model and one reaction was shown to only have a different flux range for male controls. Finally, one of the four reactions in the oxidative phosphorylation subsystem was found to have a different flux range again only in the female DCM model (Figure 5, reactions labeled with "***").

4. Discussion

In this study, cardiac sex differences in the energy metabolism of DCM patients were investigated using GSEA and context-specific GEMs. GSEA revealed that the main enriched pathways in male and female DCM patients compared to healthy controls belonged to signal transduction, immune system response and energetics and metabolism. Based on these preliminary findings, it was decided to further investigate the exact sex differences in energy metabolism using GEMs. First analysis showed that the female DCM patient model had more active pathways belonging mostly to fatty acid oxidation (FAO), glutamate metabolism and glycolysis. These findings were then further confirmed using Flux Variability Analysis (FVA), as some reactions only carried flux in the female DCM model. Additionally, FVA revealed that the energy metabolism of male DCM patients was more similar to females, implying a possible 'feminization' of the male heart in DCM.

4.1. Increased number of metabolic pathways in female DCM patients and metabolic feminization of the male DCM heart

The model overview and FVA revealed, that some reactions were only retained or only carried flux in the female DCM model. This could suggest that female metabolism is more altered in DCM which could be in accordance with the findings by Haddad et al. (2008) [8]. The researchers showed that in females, differentially expressed genes in DCM are mainly related to energy metabolism or to transcription and translation, whereas differentially expressed genes in males with DCM were mainly related to muscular contraction. However, further comparison of the results obtained from the current study and that performed by Haddad et al. (2008) is needed to determine if the genes found to be differentially expressed in females by Haddad et al. are related to the reactions that were found to be only active in the female DCM model obtained in this study.

A further observation of FVA results was that some reactions only had a different flux range in male controls, but could carry the same fluxes in other models, which could indicate that male energy metabolism in DCM starts to resemble that of females. This would be in line with the research by Alexander et al. (2010) [12], that found evidence for metabolic 'feminization' of cardiac tissue in males with DCM. However, it needs to be stressed that the results of the aforementioned paper were found to be significant only in metabolites not strictly associated with energy metabolism, such as cortisol and androgen. Nonetheless, from the data showed here, it is possible to speculate that a similar mechanism might occur also in relation to energy production.

An alternative explanation for the possibly observed 'feminization' of the male DCM heart could be that male androgen levels decrease with age, ultimately making male metabolism more similar to that of females [30]. However, as no significant difference was found in the age distribution between males in the control and the DCM group, this effect should be accounted for.

4.2. Possible FSS Results

While no results were obtained from the Flux Space Sampling, two hypotheses on the expected results were formulated based on the findings made from the model overviews and FVA. One of the results that was obtained, was that reactions that are active in females with DCM did not carry flux in any of the other models. In other words, in females with DCM, more reactions were active than in males. This could mean that more metabolic pathways are activated in females with DCM. For FSS, it would therefore be expected that either all these pathways will be activated at the same time(Figure 6B), or a different reaction

will be activated per individual run (Figure 6C). All pathways being active simultaneously would result in a lower mean flux per reaction for females with DCM compared to all other models, whereas a different reaction being activated each run would result in a higher standard deviation (Figure 6).

4.3. Discrepancies between GSEA and GEM results

From the results obtained from the GSEA, it was observed that some pathways related to cardiac energy metabolism (e.g., pyruvate metabolism, glycolysis) were only enriched in either males or females. Therefore, it was expected that these differences could also be seen in the constructed GEMs. However, most of the reactions of the investigated subsystems did not show any differences between all models in the possible flux ranges they could carry. A possible explanation for this observation is that most of the reactions belonging to energy metabolism might be associated with housekeeping genes (i.e., genes that are essential for normal cell functioning and maintenance). As these genes would be expressed similarly across all four conditions, their associated reactions were probably also retained similarly in the obtained models.

Additionally, the GIMME algorithm requires the definition of an objective function, which was set to ATP production in the current study. As only a few pathways exist to generate ATP and all models needed to retain these pathways to fulfill the objective function, any potential differences between the four conditions were possibly further obliterated. Therefore, it would be interesting to determine in future research, if more differences between the models can be observed when using other algorithms that do not require the formulation of an objective function to construct the models.

5. Conclusions and future developments

Using GSEA and context-specific GEMs, this study found evidence for a higher activation of metabolic pathways in females with DCM than males, and for 'feminization' of metabolic function in males with DCM. However, the interpretation of these results is limited by the fact that no *in vivo* studies exist that investigated sex differences in cardiac energy metabolism, which shows the importance of more studies being conducted in this area.

An additional limitation of this study is the way in which the context specific GEMs were constructed. This disadvantage is intrinsic to the GIMME algorithm, which requires the user to set an arbitrary threshold in order to determine which reactions are deemed to be active in the model. Here, the threshold was decided taking into consideration previous

studies conducted on similar topics. However, it cannot be ruled out that choosing a different value would lead to different results from the ones showed here.

Finally, as a future development to this study, a successful execution of Flux Space Sampling analysis will be performed. Since this technique does not introduce any bias concerning an objective function for the cell, we believe novel insights on the mechanisms regulating sex differences in cardiac energy metabolism will be achieved.

Supplementary Materials: Available below.

Author Contributions: Authors contributed equally to this work.

Funding: This research received no external funding

Data Availability Statement: RNA sequencing data of the left ventricle from non-failing donors and heart failure samples from the MAGNet consortium at https://www.ncbi.nlm.nih.gov/geo/query/acc.cgi?acc=GSE141910. For other data contact the authors.

Acknowledgments: Special thanks to our advisors Dr. Michiel Adriaens and Dr. Aaron Isaacs.

Conflicts of Interest: The authors declare no conflict of interest.

References

1. Schultheiss, H.P.; Fairweather, D.; Caforio, A.L.; Escher, F.; Hershberger, R.E.; Lipshultz, S.E.; Liu, P.P.; Matsumori, A.; Mazzanti, A.; McMurray, J.; et al. Dilated cardiomyopathy. *Nature reviews Disease primers* **2019**, *5*, 1–19.
2. Sinagra, G.; Merlo, M.; Pinamonti, B., Eds. *Dilated Cardiomyopathy*; Springer International Publishing, 2019. doi:10.1007/978-3-030-13864-6.
3. Jain, A.; Norton, N.; Bruno, K.A.; Cooper, L.T.; Atwal, P.S.; Fairweather, D. Sex Differences, Genetic and Environmental Influences on Dilated Cardiomyopathy. *Journal of Clinical Medicine* **2021**, *10*, 2289.
4. Rapezzi, C.; Arbustini, E.; Caforio, A.L.P.; Charron, P.; Gimeno-Blanes, J.; Helio, T.; Linhart, A.; Mogensen, J.; Pinto, Y.; Ristic, A.; et al. Diagnostic work-up in cardiomyopathies: bridging the gap between clinical phenotypes and final diagnosis. A position statement from the ESC Working Group on Myocardial and Pericardial Diseases. *European Heart Journal* **2012**, *34*, 1448–1458. doi:10.1093/eurheartj/ehs397.
5. Hershberger, R.E.; Hedges, D.J.; Morales, A. Dilated cardiomyopathy: the complexity of a diverse genetic architecture. *Nature Reviews Cardiology* **2013**, *10*, 531–547. doi:10.1038/nrcardio.2013.105.
6. Weintraub, R.G.; Semsarian, C.; Macdonald, P. Dilated cardiomyopathy. *The Lancet* **2017**, *390*, 400–414.
7. Fairweather, D.; Cooper Jr, L.T.; Blauwet, L.A. Sex and gender differences in myocarditis and dilated cardiomyopathy. *Current problems in cardiology* **2013**, *38*, 7–46.
8. Haddad, G.E.; Saunders, L.J.; Crosby, S.D.; Carles, M.; Del Monte, F.; King, K.; Bristow, M.R.; Spinale, F.G.; Macgillivray, T.E.; Semigran, M.J.; et al. Human cardiac-specific cDNA array for idiopathic dilated cardiomyopathy: sex-related differences. *Physiological genomics* **2008**, *33*, 267–277.
9. Sheppard, R.; Bedi, M.; Kubota, T.; Semigran, M.J.; Dec, W.; Holubkov, R.; Feldman, A.M.; Rosenblum, W.D.; McTiernan, C.F.; McNamara, D.M.; et al. Myocardial expression of fas and recovery of left ventricular function in patients with recent-onset cardiomyopathy. *Journal of the American College of Cardiology* **2005**, *46*, 1036–1042.
10. Karwi, Q.G.; Uddin, G.M.; Ho, K.L.; Lopaschuk, G.D. Loss of metabolic flexibility in the failing heart. *Frontiers in cardiovascular medicine* **2018**, *5*, 68.
11. Karlstädt, A.; Fliegner, D.; Kararigas, G.; Ruderisch, H.S.; Regitz-Zagrosek, V.; Holzhütter, H.G. CardioNet: A human metabolic network suited for the study of cardiomyocyte metabolism. *BMC Systems Biology* **2012**, *6*, 114. doi:10.1186/1752-0509-6-114.
12. Alexander, D.; Lombardi, R.; Rodriguez, G.; Mitchell, M.M.; Marian, A.J. Metabolomic distinction and insights into the pathogenesis of human primary dilated cardiomyopathy. *European journal of clinical investigation* **2011**, *41*, 527–538.
13. Shlomi, T.; Cabili, M.N.; Herrgård, M.J.; Palsson, B.Ø.; Ruppin, E. Network-based prediction of human tissue-specific metabolism. *Nature biotechnology* **2008**, *26*, 1003–1010.
14. Varma, A.; Palsson, B.O. Stoichiometric flux balance models quantitatively predict growth and metabolic by-product secretion in wild-type Escherichia coli W3110. *Applied and environmental microbiology* **1994**, *60*, 3724–3731.
15. https://www.ncbi.nlm.nih.gov/bioproject/PRJNA595151.
16. Wickham, H.; Averick, M.; Bryan, J.; Chang, W.; McGowan, L.D.; François, R.; Grolemund, G.; Hayes, A.; Henry, L.; Hester, J.; et al. Welcome to the tidyverse. *Journal of Open Source Software* **2019**, *4*, 1686. doi:10.21105/joss.01686.
17. W, S.; H, R.; M, S.; D, W.; J, S. pcaMethods - a Bioconductor package providing PCA methods for incomplete data. *Bioinformatics* **2007**, *23*.
18. Robinson, M.D.; McCarthy, D.J.; Smyth, G.K. edgeR: a Bioconductor package for differential expression analysis of digital gene expression data. *Bioinformatics* **2010**, *26*, 139–140.
19. Ritchie, M.E.; Phipson, B.; Wu, D.; Hu, Y.; Law, C.W.; Shi, W.; Smyth, G.K. limma powers differential expression analyses for RNA-sequencing and microarray studies. *Nucleic acids research* **2015**, *43*, e47–e47.
20. Robinson, M.D.; Oshlack, A. A scaling normalization method for differential expression analysis of RNA-seq data. *Genome Biology* **2010**, *11*, R25. doi:10.1186/gb-2010-11-3-r25.
21. Smyth, G.K.; Ritchie, M.; Thorne, N.; Wettenhall, J.; Shi, W.; Hu, Y. *limma: Linear Models for Microarray and RNA-Seq Data User's Guide*; Bioinformatics Division, The Walter and Eliza Hall Institute of Medical Research: Melbourne, Australia, 2002.
22. Law, C.W.; Chen, Y.; Shi, W.; Smyth, G.K. voom: precision weights unlock linear model analysis tools for RNA-seq read counts. *Genome Biology* **2014**, *15*, R29. doi:10.1186/gb-2014-15-2-r29.
23. Durinck, S.; Moreau, Y.; Kasprzyk, A.; Davis, S.; Moor, B.D.; Brazma, A.; Huber, W. BioMart and Bioconductor: a powerful link between biological databases and microarray data analysis. *Bioinformatics* **2005**, *21*, 3439–3440. doi:10.1093/bioinformatics/bti525.
24. Orth, J.D.; Thiele, I.; Palsson, B.Ø. What is flux balance analysis? *Nature biotechnology* **2010**, *28*, 245–248.
25. Becker, S.A.; Palsson, B.O. Context-specific metabolic networks are consistent with experiments. *PLoS computational biology* **2008**, *4*, e1000082.
26. Heirendt, L.; Arreckx, S.; Pfau, T.; Mendoza, S.N.; Richelle, A.; Heinken, A.; Haraldsdóttir, H.S.; Wachowiak, J.; Keating, S.M.; Vlasov, V.; et al. Creation and analysis of biochemical constraint-based models using the COBRA Toolbox v. 3.0. *Nature protocols* **2019**, *14*, 639–702.
27. Brunk, E.; Sahoo, S.; Zielinski, D.C.; Altunkaya, A.; Dräger, A.; Mih, N.; Gatto, F.; Nilsson, A.; Gonzalez, G.A.P.; Aurich, M.K.; et al. Recon3D enables a three-dimensional view of gene variation in human metabolism. *Nature biotechnology* **2018**, *36*, 272–281.
28. Noronha, A.; Daníelsdóttir, A.D.; Gawron, P.; Jóhannsson, F.; Jónsdóttir, S.; Jarlsson, S.; Gunnarsson, J.P.; Brynjólfsson, S.; Schneider, R.; Thiele, I.; et al. ReconMap: an interactive visualization of human metabolism. *Bioinformatics* **2017**, *33*, 605–607.
29. Mahadevan, R.; Schilling, C.H. The effects of alternate optimal solutions in constraint-based genome-scale metabolic models. *Metabolic engineering* **2003**, *5*, 264–276.

30. Mohr, B.A.; Guay, A.T.; O'Donnell, A.B.; McKinlay, J.B. Normal, bound and nonbound testosterone levels in normally ageing men: results from the Massachusetts Male Ageing Study. *Clinical endocrinology* **2005**, *62*, 64–73.

Figures and tables

Table 1. Overview of sample characteristics.

Factor		Female (n = 155)			Male (n = 177)		
		Donor (n = 89)	DCM (n = 66)	Sig.	Donor (n = 77)	DCM (n = 100)	Sig.
n Ethnicity (%)	African-American	23 (25.8%)	36 (54.5%)	**<.001** [1]	21 (27.3%)	41 (41.0%)	.06 [1]
	Caucasian	66 (74.2%)	30 (45.5%)		56 (72.7%)	59 (59.0%)	
Mean Age in years (SD)		59.0 (12.5)	51.1 (11.7)	**<.001** [2]	52.6 (12.2)	52.7 (9.8)	.8 [2]

Significant differences between control and DCM are highlighted in bold.
[1] ANOVA independent t-test with assumed equal variance
[2] Chi-square test

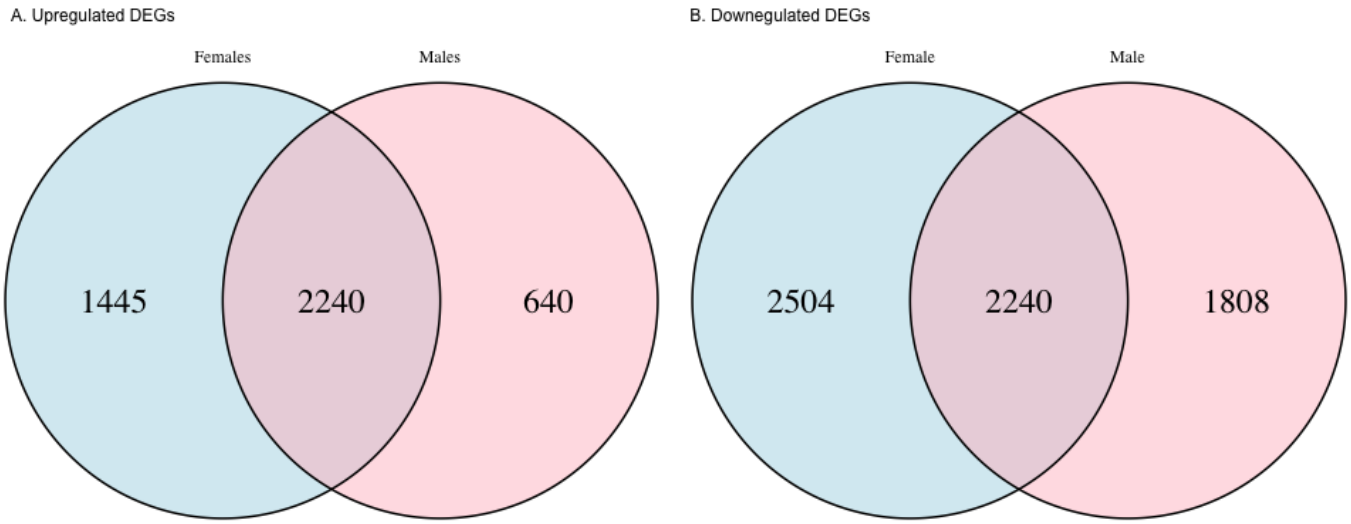

Figure 1. The Venn diagrams of differentially expressed genes (DEGs) after filtering in female DCM vs. Donor samples and male DCM vs. Donor samples. (**A**) Upregulated DEGs. (**b**) Downregulated DEGs.

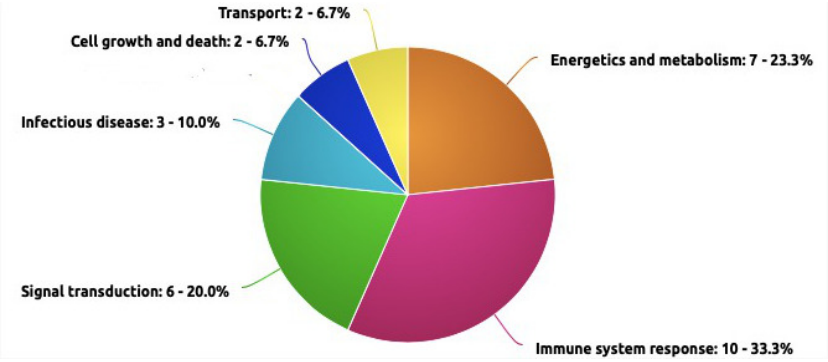

((**a**)) Male enriched pathways, KEGG

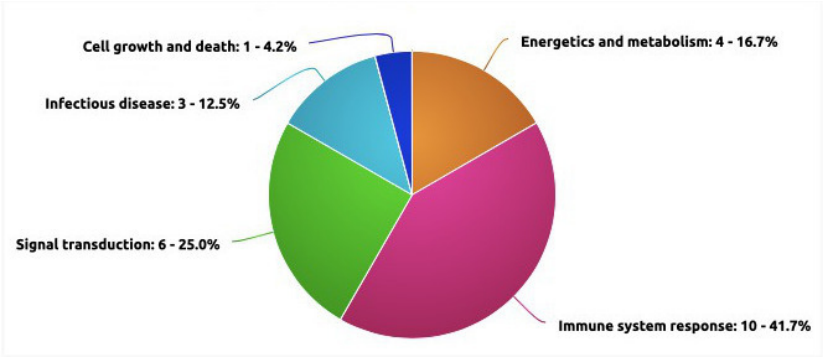

((**b**)) Female enriched pathways, KEGG

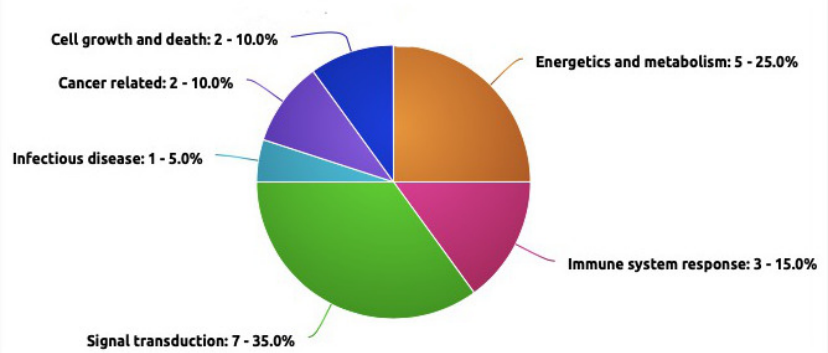

((**c**)) Male enriched pathways, WP

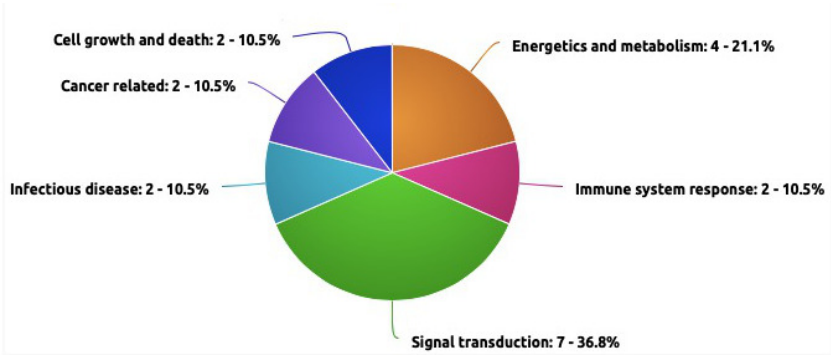

((**d**)) Female enriched pathways, WP

Figure 2. Piechart of enriched pathways grouped into categories. For (**a**) males and (**b**) females from KEGG database and (**c**) males and (**d**) females from WikiPathways (WP).

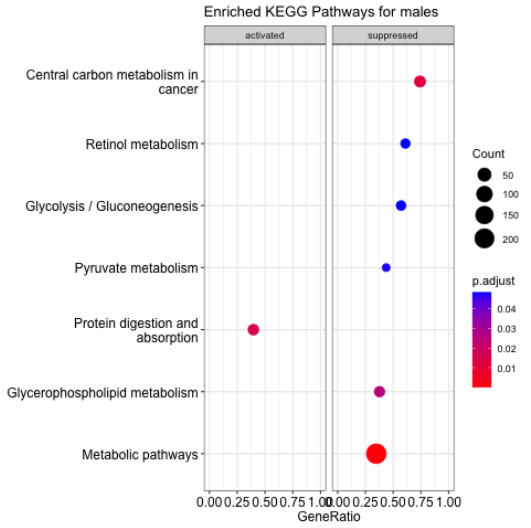

((**a**)) KEGG males

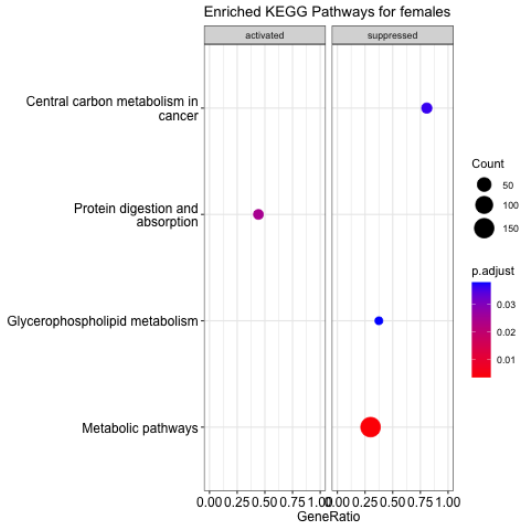

((**b**)) KEGG females

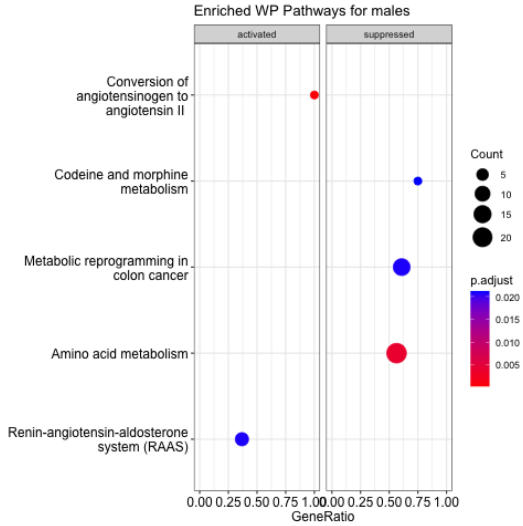

((**c**)) WP males

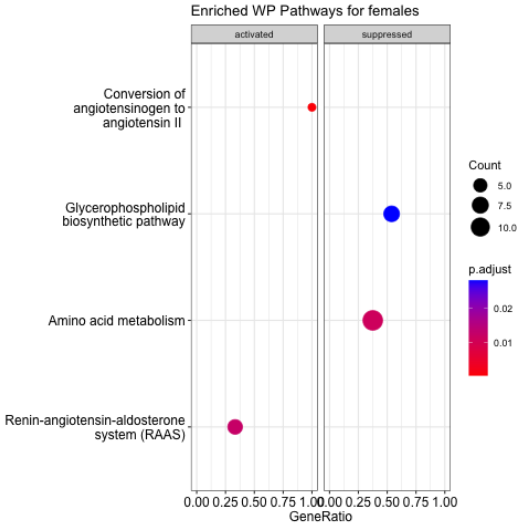

((**d**)) WP females

Figure 3. Dotplots of enriched pathways related to energetics and metabolism for (**a**) males and (**b**) females using KEGG database and (**c**) males and (**d**) females using WikiPathways (WP).

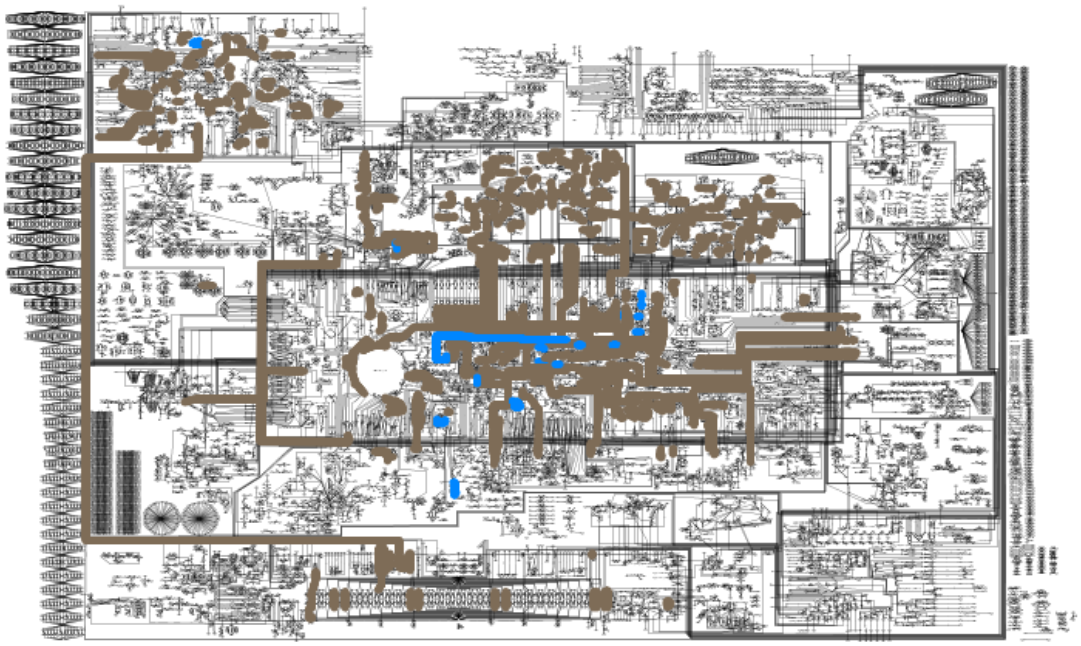

((**a**)) Control

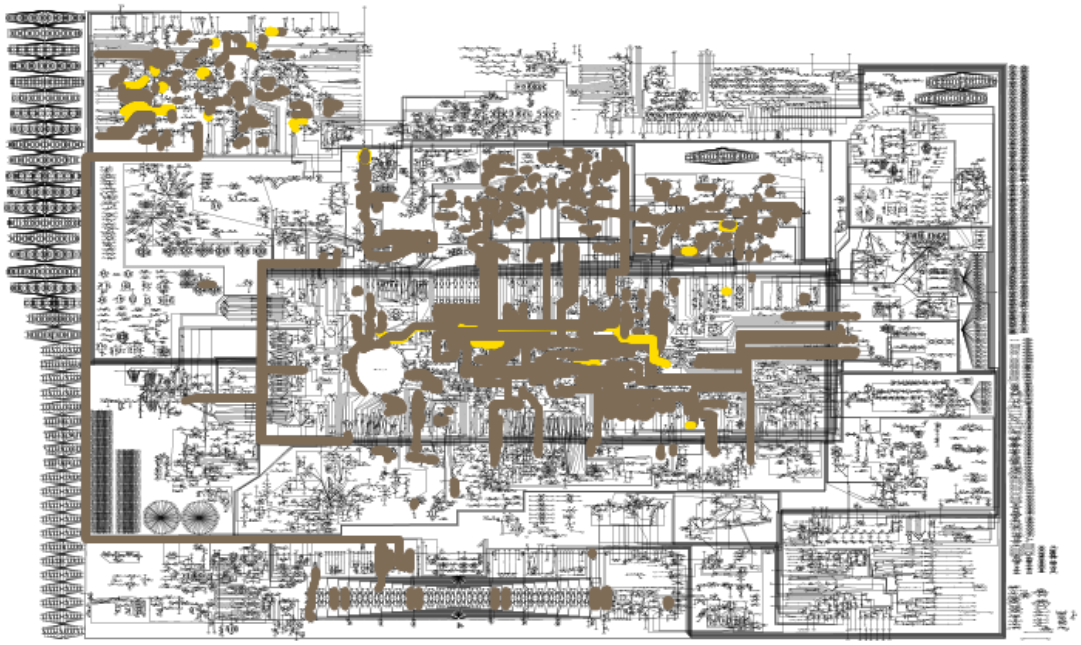

((**b**)) DCM

Figure 4. Recon3 FBA overview of the of active metabolic reactions present in (**a**) control female vs. male models and (**b**) DCM female vs. male models displayed only for subsystems of interest. Yellow reactions are only active in female models, blue only in male models and brown are active in both models.

Figure 5. Range barplots of the reactions with different fluxes only in control groups or DCM groups.
* Fatty acid oxidation subsystem
** Pyruvate metabolism subsystem
*** Oxidative phosphorylation subsystem

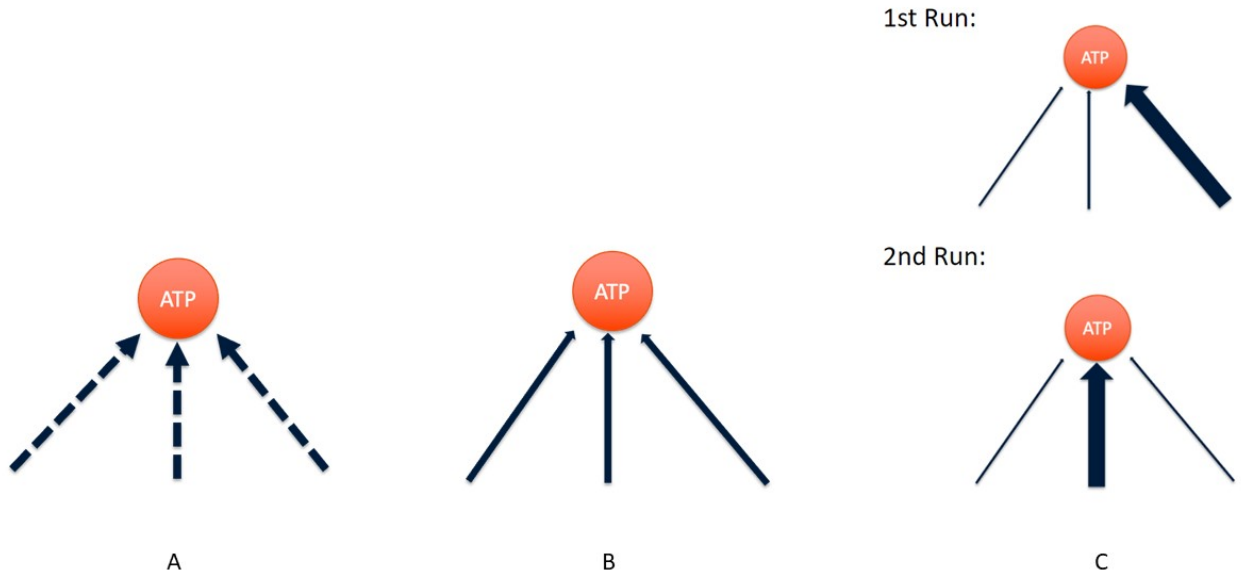

Figure 6. Illustration of the expected FSS results for females with DCM. (**A**) Multiple pathways (arrows) exist to generate ATP. (**B**) One hypothesis is that all reactions are active in females with DCM, resulting in a lower mean flow per reaction compared to all other models. (**C**) Another hypothesis is that a different reaction is activated per simulation. This would result in a higher standard deviation per reaction in females with DCM.

Supplementary materials

Table 2. List of enriched pathways and their assigned categories for males and females with KEGG and WikiPathways (WP) databases. Pathways in bold were found in only males or only females. Enrichment score <0 means downregulated pathway and >0 upregulated.

Pathway name	Category	Database	Enrichment score
A. Enriched pathways for males			
Photodynamic therapy-induced HIF-1 survival signaling	Cancer related pathway	WP	-0,63656
Retinoblastoma gene in cancer		WP	-0,39086
p53 signaling pathway	Cell cycle, growth and death	KEGG	-0,41611
Ribosome biogenesis in eukaryotes		KEGG	-0,51206
Ferroptosis		WP	-0,53704
Parkin-ubiquitin proteasomal system pathway		WP	-0,48732
Amino acid metabolism	Energetics and metabolism	WP	-0,52561
Central carbon metabolism in cancer		KEGG	-0,51474
Codeine and morphine metabolism		WP	-0,90915
Conversion of angiotensinogen to angiotensin II		WP	0,98906
Glycerophospholipid metabolism		KEGG	-0,43205
Glycolysis / Gluconeogenesis		KEGG	-0,51559
Metabolic pathways		KEGG	-0,24899
Metabolic reprogramming in colon cancer		WP	-0,56326
Protein digestion and absorption		KEGG	0,50981
Pyruvate metabolism		KEGG	-0,55946
Renin-angiotensin-aldosterone system (RAAS)		WP	0,65803
Retinol metabolism		KEGG	-0,54922

Antigen processing and presentation	Immune system response	KEGG	0,50857
Complement and coagulation cascades		KEGG	-0,44153
Complement system		WP	-0,44322
Graft-versus-host disease		KEGG	0,70261
Hematopoietic cell lineage		KEGG	0,45854
Microglia pathogen phagocytosis pathway		WP	-0,56599
Natural killer cell mediated cytotoxicity		KEGG	0,43204
Overview of proinflammatory and profibrotic mediators		WP	0,54534
Primary immunodeficiency		KEGG	0,68987
Rheumatoid arthritis		KEGG	0,46606
Th1 and Th2 cell differentiation		KEGG	0,56460
Th17 cell differentiation		KEGG	0,48355
Type I diabetes mellitus		KEGG	0,65608
Malaria	Infectious disease	KEGG	0,51706
Pathogenic Escherichia coli infection		KEGG	-0,31115
Pathogenic Escherichia coli infection		WP	-0,61327
Salmonella infection		KEGG	-0,32702
Cell adhesion molecules	Signal transduction	KEGG	0,45489
Cytokine-cytokine receptor interaction		KEGG	0,38513
EGF/EGFR signaling pathway		WP	-0,34510
Glucocorticoid receptor pathway		WP	-0,51118
Hedgehog signaling pathway		KEGG	0,57606
HIF-1 signaling pathway		KEGG	-0,43030
IL-10 anti-inflammatory signaling pathway		WP	-0,86061
Modulators of TCR signaling and T cell activation		WP	0,56157
Neuroactive ligand-receptor interaction		KEGG	0,37304
Neuroinflammation and glutamatergic signaling		WP	-0,36452
Nuclear receptors meta-pathway		WP	-0,35924

Oncostatin M signaling pathway		WP	-0,49310
Viral protein interaction with cytokine and cytokine receptor		KEGG	0,48804
Gap junction	Transport	KEGG	-0,43969
Phagosome		KEGG	-0,33269

B. Enriched pathways for females

Cancer immunotherapy by PD-1 blockade	Cancer related pathways	WP	0,70739
Retinoblastoma gene in cancer		WP	-0,40561
DNA IR-damage and cellular response via ATR	Cell cycle, growth and death	WP	-0,46408
Ferroptosis		WP	-0,51615
Ribosome biogenesis in eukaryotes		KEGG	-0,51337
Amino acid metabolism	Energetics and metabolism	WP	-0,51265
Central carbon metabolism in cancer		KEGG	-0,48205
Conversion of angiotensinogen to angiotensin II		WP	0,98951
Glycerophospholipid biosynthetic pathway		WP	-0,66173
Glycerophospholipid metabolism		KEGG	-0,40776
Metabolic pathways		KEGG	-0,20461
Protein digestion and absorption		KEGG	0,47826
Renin-angiotensin-aldosterone system (RAAS)		WP	0,65435
Allograft rejection	Immune system response	KEGG	0,59531
Allograft rejection		WP	0,48278
Antigen processing and presentation		KEGG	0,54292
Chemokine signaling pathway		KEGG	0,43477
Graft-versus-host disease		KEGG	0,72512
Hematopoietic cell lineage		KEGG	0,52230
Natural killer cell mediated cytotoxicity		KEGG	0,48315

Overview of proinflammatory and profibrotic mediators		WP	0,61885
Primary immunodeficiency		KEGG	0,78296
Th1 and Th2 cell differentiation		KEGG	0,55587
Th17 cell differentiation		KEGG	0,48523
Type I diabetes mellitus		KEGG	0,67954
African trypanosomiasis	Infectious disease	KEGG	0,64204
Pathogenesis of SARS-CoV-2 mediated by nsp9-nsp10 complex		WP	0,68121
Pathogenic Escherichia coli infection		KEGG	-0,32288
Pathogenic Escherichia coli infection		WP	-0,68316
Salmonella infection		KEGG	-0,36207
Cell adhesion molecules	Signal transduction	KEGG	0,50240
Cytokine-cytokine receptor interaction		KEGG	0,41625
EGF/EGFR signaling pathway		WP	-0,38066
EGFR tyrosine kinase inhibitor resistance		KEGG	-0,45836
EGFR tyrosine kinase inhibitor resistance		WP	-0,43585
Glucocorticoid receptor pathway		WP	-0,56283
HIF-1 signaling pathway		KEGG	-0,46193
Insulin signaling		WP	-0,35619
Modulators of TCR signaling and T cell activation		WP	0,61235
Neuroactive ligand-receptor interaction		KEGG	0,37968
Nuclear receptors meta-pathway		WP	-0,37755
Oncostatin M signaling pathway		WP	-0,54411
Viral protein interaction with cytokine and cytokine receptor		KEGG	0,55657

Table 3. Overview of properties of the obtained context-specific GEMs.

	Female		Male	
	Control	DCM	Control	DCM
Reactions	8513	9129	8574	8824
Metabolites	7498	7690	7536	7592
Metabolites (unique)	3808	3872	3826	3851
Compartments (unique)	9	9	9	9
Genes (unique)	3290	3290	3290	3290
Deadends	3012	2767	3023	2899
Size of S	7498;8513	7690;9129	7536;8574	7592;8824
Rank of S	6717	6995	6748	6851
Percentage nz	0.00049909	0.00049647	0.00049692	0.00049767

Table 4. Overview of performed sanity checks on the obtained GEMs. Results were the same across all models.

	Female		Male	
Test	Control	DCM	Control	DCM
fastLeakTest1	Leak free			
Exchanges, sinks, and demands have lb = 0, except H2O	Model does not produce energy from water			
Exchanges, sinks and demands have lb = 0, except H2O and O2	Model does not produce energy from water and oxygen			
Exchanges, sinks, and demands have lb = 0, allow DM_atp_c to be reversible	Model does not produce matter when ATP demand is reversed			
Exchanges, sinks, and demands have lb = 0, test flux through DM_h[m](max)	Model has no flux through h[m] demand (max)			
Exchanges, sinks, and demands have lb = 0, test flux through DM_h[c](max)	Model has no flux through h[c] demand (max)			
ATP yield	Model does not produce too much ATP demand from Glc			
Check duplicated reactions	No duplicated reactions in model			
Check empty columns in rxnGeneMat	Empty columns in rxnGeneMat			
Check that demand reactions have a lb >=0	No demand reaction can have flux in backward reaction			
Check whether singleGeneDeletion runs smoothly	singleGeneDeletion finished without problems			
Check flux consistency	Model is not flux consistent			

Table 5. Differences in active metabolic reactions between DCM female vs. male and Donor female vs. male GIMME models.

Reaction name	Subsystem	Description
A. Active reactions in both males and females in DCM and only in males in control		
LGTHL	Pyruvate metabolism	Lactoylglutathione Lyase
GTHOM	Glutamate metabolism	Glutathione Oxidoreductase
GTHO	Glutamate metabolism	Glutathione Oxidoreductase
CBPSAM	Glutamate metabolism	Carbamoyl-Phosphate Synthase (Ammonia), Mitochondrial
RE1517X	Fatty acid oxidation	RE1517X
FAOXC225M	Fatty acid oxidation	Isomerization (C22:5), Mitochondrial
FAOXC184M	Fatty acid oxidation	Isomerization of (C18:4), Mitochondrial
FAOXC163GM	Fatty acid oxidation	Isomerization (C16:3), Mitochondrial
FAOXTC122M	Fatty acid oxidation	Isomerization Trans (C12:2), Mitochondrial
FAOXC122M	Fatty acid oxidation	Isomerization (C12:2), Mitochondrial
FAOXC101M	Fatty acid oxidation	Isomerization (C10:1), Mitochondrial
FAOXC185M	Fatty acid oxidation	Isomerization (C18:5), Mitochondrial
FAOXC226M	Fatty acid oxidation	Isomerization (C22:6), Mitochondrial
FAOXC123M	Fatty acid oxidation	Isomerization (C12:3), Mitochondrial
FAOXC61M	Fatty acid oxidation	Isomerization (C6:1), Mitochondrial
FAOXC102M	Fatty acid oxidation	Isomerization (C10:2), Mitochondrial
FAOXC164M	Fatty acid oxidation	Fatty Acid Beta Oxidation (C16:4->C16:3), Peroxisomal
DCIM	Fatty acid oxidation	Dodecenoyl-Coenzyme A Delta Isomerase
B. Active reactions in only females in DCM and non-active in control		
ACSM	Glycolysis/gluconeogenesis	Acetyl Coenzyme A Synthetase
R0355	Glycolysis/gluconeogenesis	Hexokinase
R0354	Glycolysis/gluconeogenesis	Hexokinase
DOCOSACT	Fatty acid oxidation	Activation of Docosanoic Acid for Transport
MCDM	Fatty acid oxidation	Malonyl Coenzyme A Decarboxylase, Mitochondrial
MCDP	Fatty acid oxidation	Malonyl Coenzyme A Decarboxylase Peroxisomal
MCD	Fatty acid oxidation	Malonyl Coenzyme A Decarboxylase Cytoplasmic

RE2624X	Fatty acid oxidation	Alpha-Methylacyl Coenzyme A Racemase
RE2993X	Fatty acid oxidation	2,4-Dienoyl Coenzyme A Reductase (NADPH)
RE2996X	Fatty acid oxidation	2,4-Dienoyl Coenzyme A Reductase (NADPH)
RE3195M	Fatty acid oxidation	Alpha-Methylacyl Coenzyme A Racemase
RE3083X	Fatty acid oxidation	Alpha-Methylacyl Coenzyme A Racemase
PHYHX	Fatty acid oxidation	Phytanoyl Coenzyme A Dioxygenase, Peroxisomal
FAOXC102C101x	Fatty acid oxidation	Fatty Acid Beta Oxidation (C10:2->C10:1), Peroxisomal
FAOXC103C102X	Fatty acid oxidation	Fatty Acid Beta Oxidation (C10:3->C10:2), Peroxisomal
FAOXC164C163X	Fatty acid oxidation	Fatty Acid Beta Oxidation (C16:4->C16:3), Peroxisomal
FAOXC165C164x	Fatty acid oxidation	Fatty Acid Beta Oxidation (C16:5->C16:4), Peroxisomal
FAOXC226C225x	Fatty acid oxidation	Fatty Acid Beta Oxidation (C22:6->C22:5), Peroxisomal
FAOXC160	Fatty acid oxidation	Beta Oxidation of Long Chain Fatty Acid